



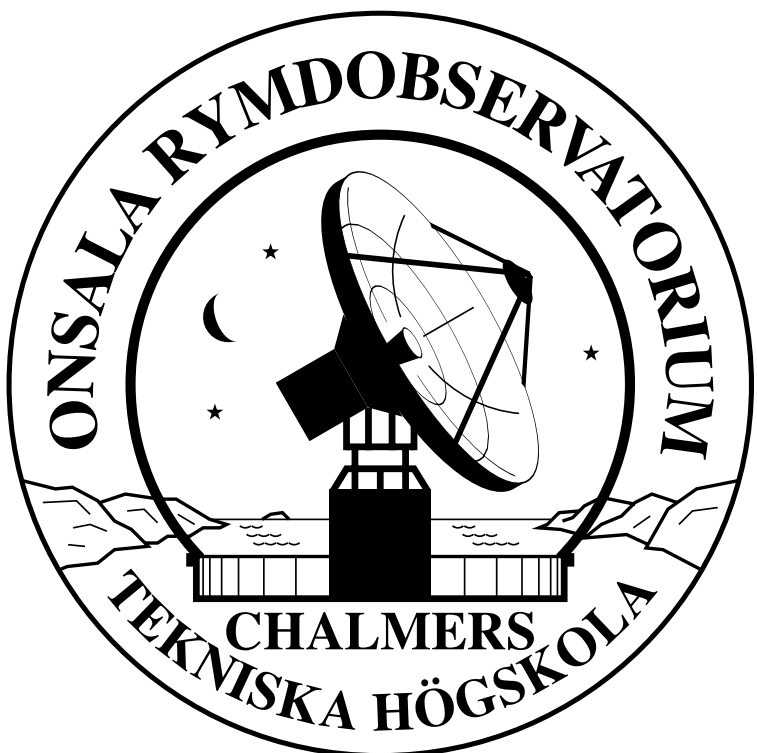
CHALMERS

# Comparison of atmospheric gradients estimated from ground-based GNSS observations and microwave radiometry

Gunnar Elgered<sup>1</sup>, Peter Forkman<sup>1</sup>, and Tong Ning<sup>2</sup>

<sup>1</sup>Chalmers University of Technology, Onsala Space Observatory, SE-439 92 Onsala, Sweden

<sup>2</sup>Lantmäteriet (Swedish Mapping, Cadastral and Land Registration Authority), SE-801 82 Gävle, Sweden



## Introduction

Since many years it is common practice to estimate horizontal linear gradients in GNSS data processing since it has a positive impact on the reproducibility of estimated geodetic parameters (Bar-Sever et al., 1998). The potential use of estimated gradients in meteorology has also been studied (Morel et al., 2015; Graffigna et al., 2019).

We have estimated linear horizontal gradients in the atmosphere using four years of data from ground-based GPS and water vapour radiometer (WVR) observations at the Onsala site on the Swedish west coast. The GPS data are from the two collocated IGS stations ONSA and ONS1.

The GPS gradients are estimated for both the ONSA and ONS1 stations using three different elevation cutoff angles: 3°, 10°, and 20° with a temporal resolution of 5 min. The WVR observations are always acquired at elevation angles > 20° to avoid emission from the ground. Approximately 100 observations spread over the sky during 15 min are used to estimate the east and the north wet gradients. For a complete description of the data processing carried out in order to derive the gradients see Elgered et al. (2019). The GPS antenna installations and the WVR are shown in Fig. 1.

In this study we focus on the wet gradients meaning that the hydrostatic gradients from the European Centre for Medium-Range Weather Forecasts (ECMWF) (Boehm and Schuh, 2007) are subtracted from the total gradients, originally estimated from the GPS data.



Fig. 1. The GNSS antenna installations ONSA (left) and ONS1 (middle) and the WVR Konrad (right).

## Characterization of gradients

The entire data set spans four years, 2013 – 2016. As seen in Fig. 2 the coverage of the gradients from GPS is almost continuous, whereas there are a few gaps in the WVR time series. In addition to the north and east components we can also study the time series of gradient amplitudes in Fig. 3 and their distribution in Fig. 4. Fig. 5 depicts all the estimated gradients in terms of their amplitudes and directions. In Fig. 3 we see that the largest gradients occur during the warmer, and wetter, part of the year.

The majority of all gradients are small and of comparable size to their formal uncertainties. Therefore, we now focus on the gradients with the largest amplitudes.

## Large gradients

Large wet gradients are not evenly distributed with angle as illustrated in Fig. 6. The GPS stations ONSA and ONS1 give, as expected, similar distributions, but only for the elevation cutoff angles of 3° and 10°. For the 20° cutoff angle the large gradients sensed by ONSA are mainly towards the south-west, whereas ONS1 gradients are mainly in the east direction. We interpret this contradiction to be due to systematic errors appearing when the geometry of the observed satellites becomes weak. This calls for further studies. Although based on the same input data, this confirms the earlier result (Elgered et al., 2019) that the GPS gradients from the 3° cutoff angle solution show the highest correlation with the WVR gradients.

Another observation is that gradients towards the south-west may be due to warm fronts from this direction and gradients towards the east may correspond to cold fronts from the west. Although this is speculative, it makes sense given that the prevailing winds are from the west and that colder air typically come from higher latitudes, i.e. warm fronts arrive from a more southern direction compared to the cold fronts.

In order to examine the cause of large wet gradients in more detail we identified the 20 largest gradient amplitudes in Fig. 3. They all happened during the period of the year beginning in April and ending in October. We expanded the time scale and plotted the north and the east gradients together with the wet zenith delay (ZWD) for the six GPS solutions, and for the WVR reference data set. A rapid change in the ZWD is an indication of the passage of a frontal system and the corresponding shift between drier and more humid air masses.

An overall result is that the passage of a weather front is the most common reason for the existence of large gradients. We note that this observation is of course only a valid at this specific location, where frontal systems pass regularly. We show three examples in Figs. 7, 8, and 9. Here we plot east and north gradients estimated by both ONSA and ONS1 data for each one of the three different elevation cutoff angles and the gradients estimated from the WVR data. Note that precipitation is often associated with frontal system and that this is the reason why WVR data are missing during some periods. The algorithm which corrects the sky brightness temperatures for liquid water drops does not hold during rain.

## Conclusions and future work

We find that estimated linear horizontal gradients are not homogeneously distributed in all directions. For the Onsala site there is a preference for east-west gradients, possibly caused by that the prevailing winds are from the west and that it is a coastal station, with the coast line oriented in the north-south direction.

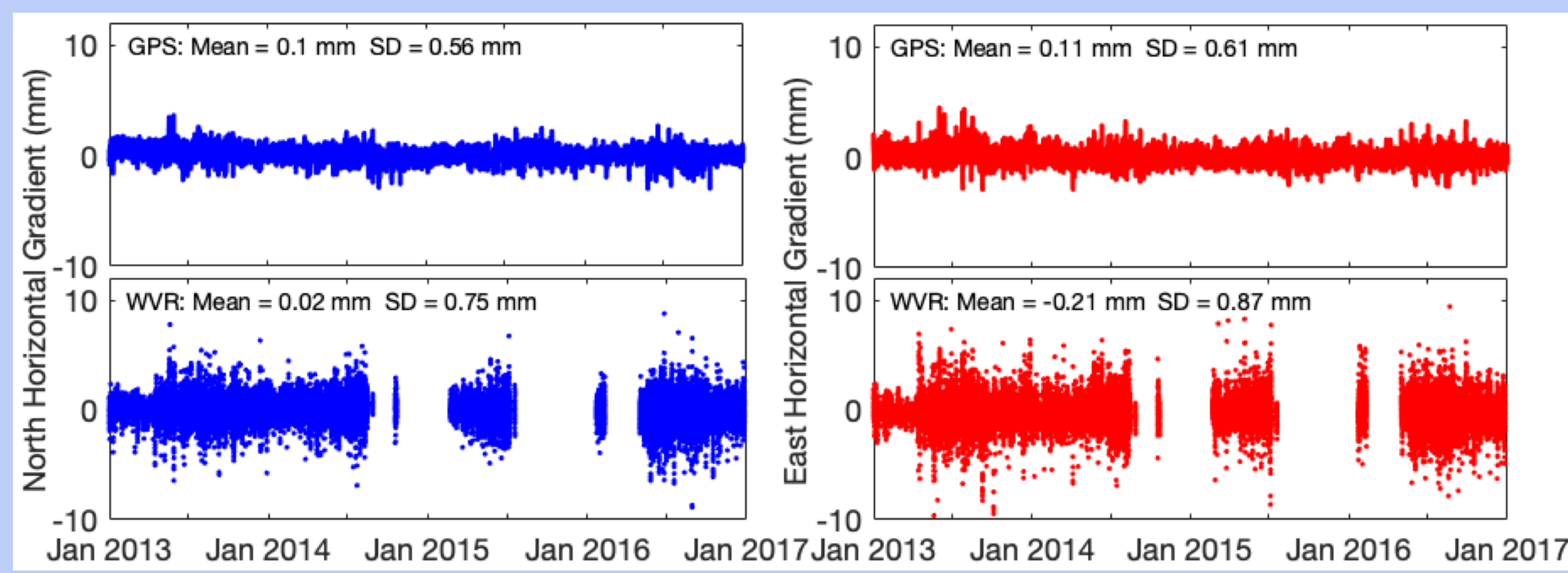


Fig. 2. Time series of estimated north (left) and east (right) wet gradients from GPS (top) and WVR (bottom). GPS gradients are from the ONSA station using a 3° elevation cutoff angle. A seasonal dependence with larger gradients during the warmer part of year is seen. The variability, presented as standard deviations (SD), are significantly larger in the WVR gradients (bottom graphs) compared to the GPS gradients. The WVR gradients are estimated independently of previous values, whereas the GPS gradients are estimated using a constraint for the temporal variability.

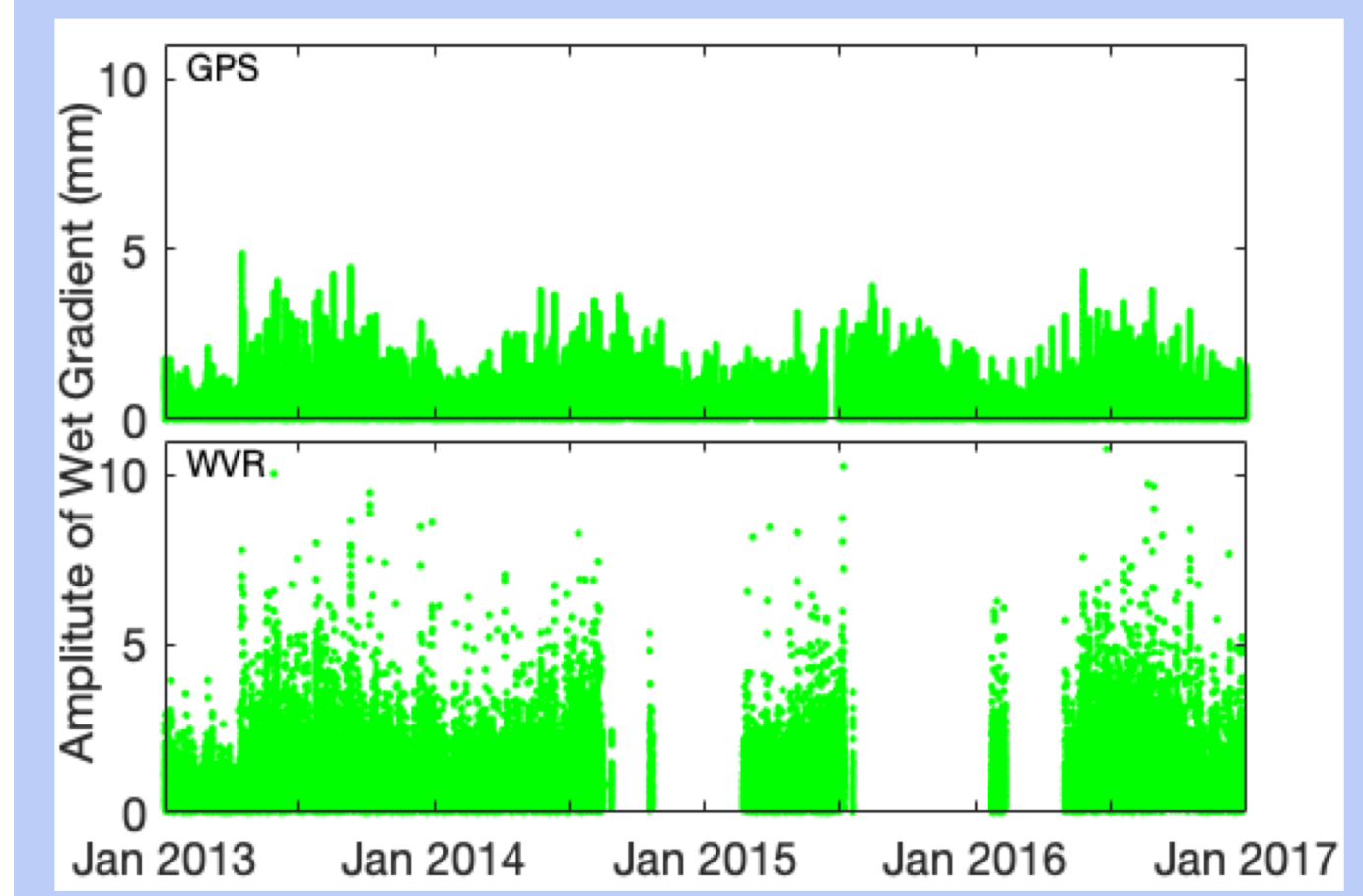


Fig. 3. Time series of the wet gradient amplitudes calculated from the data shown in Fig. 2. The relative distribution of these amplitudes are shown in Fig. 4, and in Fig. 5, where we show them as a function of their direction.

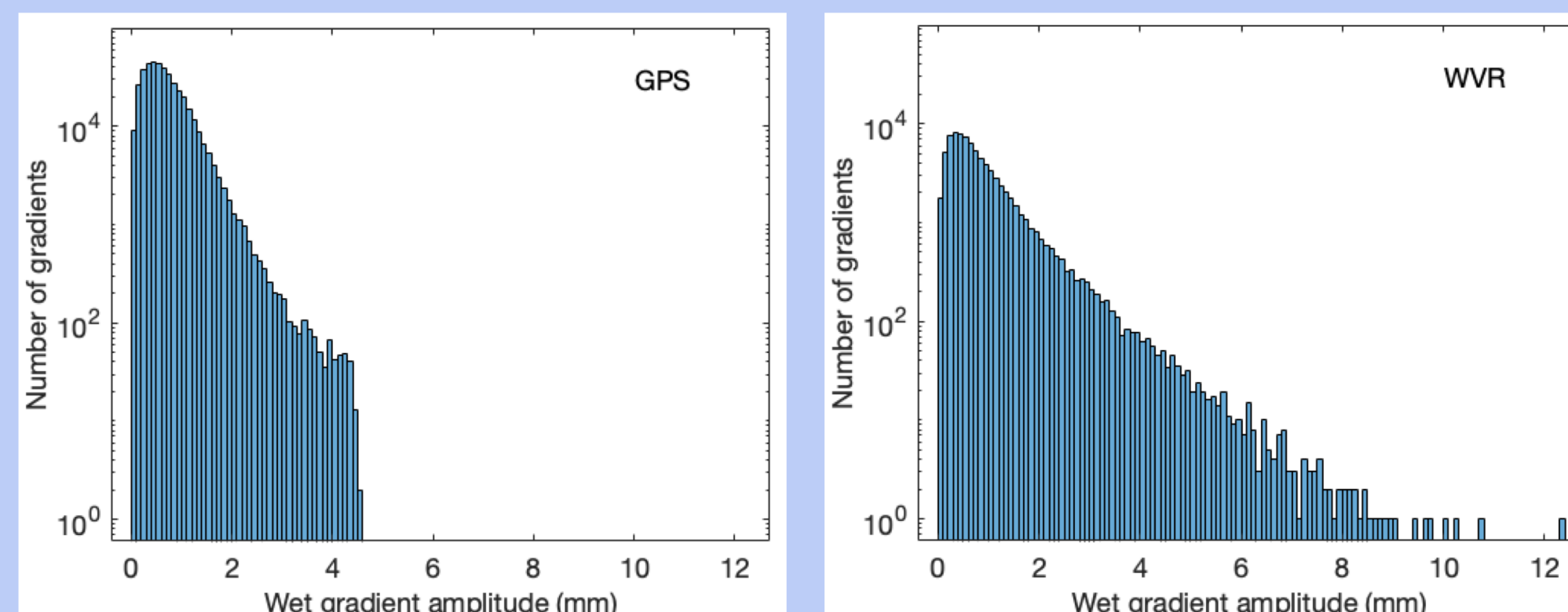


Fig. 4. Histogram of the amplitudes of wet gradients shown in Fig. 3. Note the logarithmic scale on the y-axis. The mean gradient amplitude for the whole data set is 0.51 mm for the ONSA station using the 3° cutoff angle (left graph) and increases to 0.75 mm for the 20° cutoff angle. The mean gradient amplitude for the WVR data (right graph) is 0.87 mm (Elgered et al., 2019).

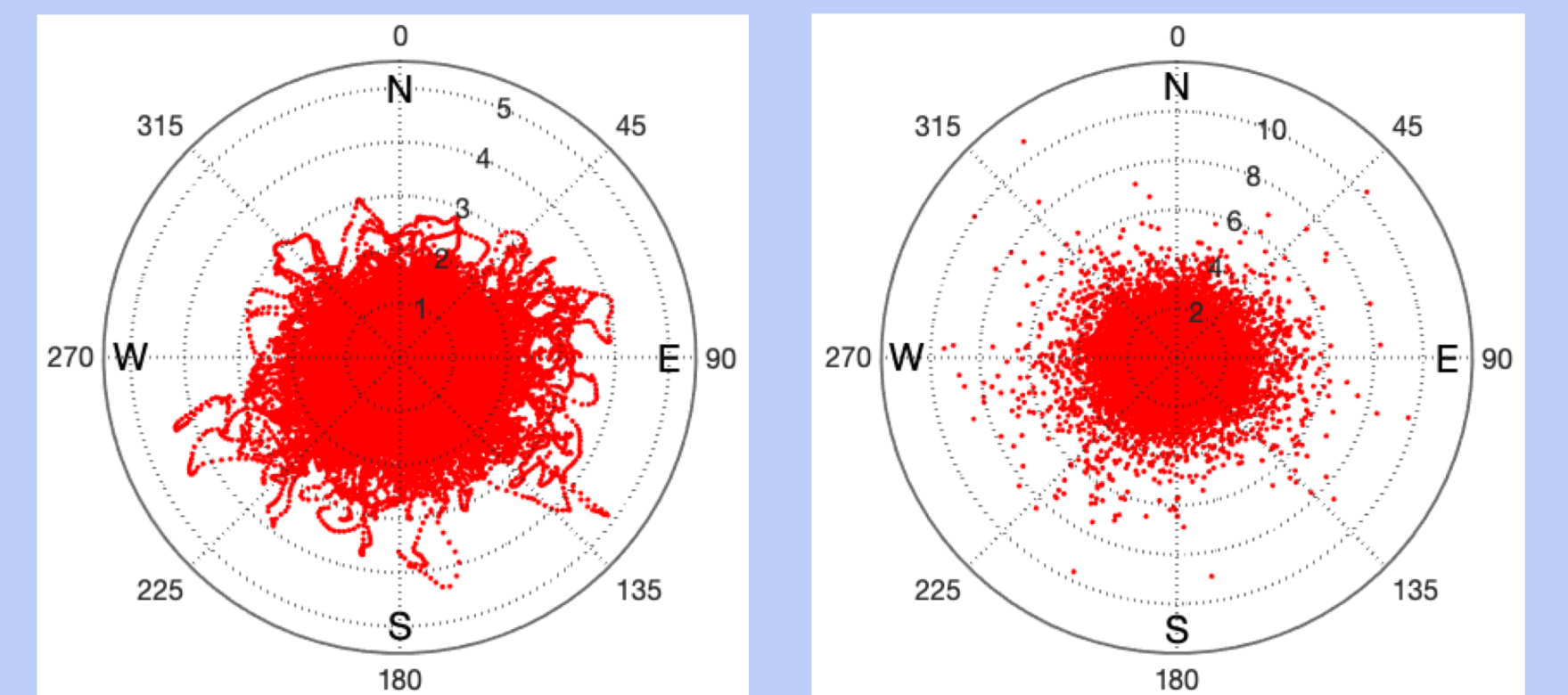


Fig. 5. Distribution of 408,090 wet gradient amplitudes, estimated every 5 min, from the ONSA station using a 3° cutoff angle (left) and 81,625 wet gradients, estimated every 15 min, from the WVR (right). Note the different radial scales.

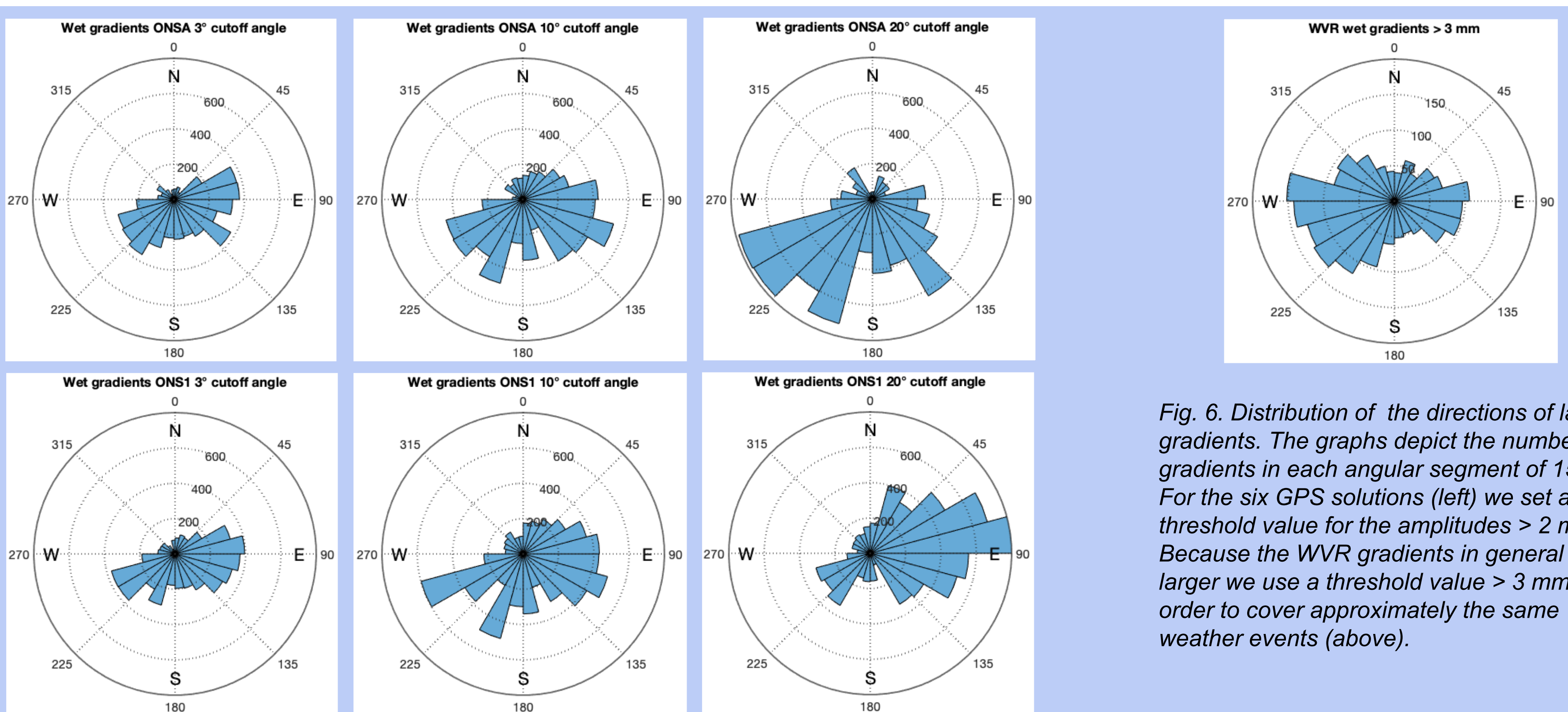


Fig. 6. Distribution of the directions of large gradients. The graphs depict the number of gradients in each angular segment of 15°. For the six GPS solutions (left) we set a threshold value for the amplitudes > 2 mm. Because the WVR gradients in general are larger we use a threshold value > 3 mm in order to cover approximately the same weather events (above).

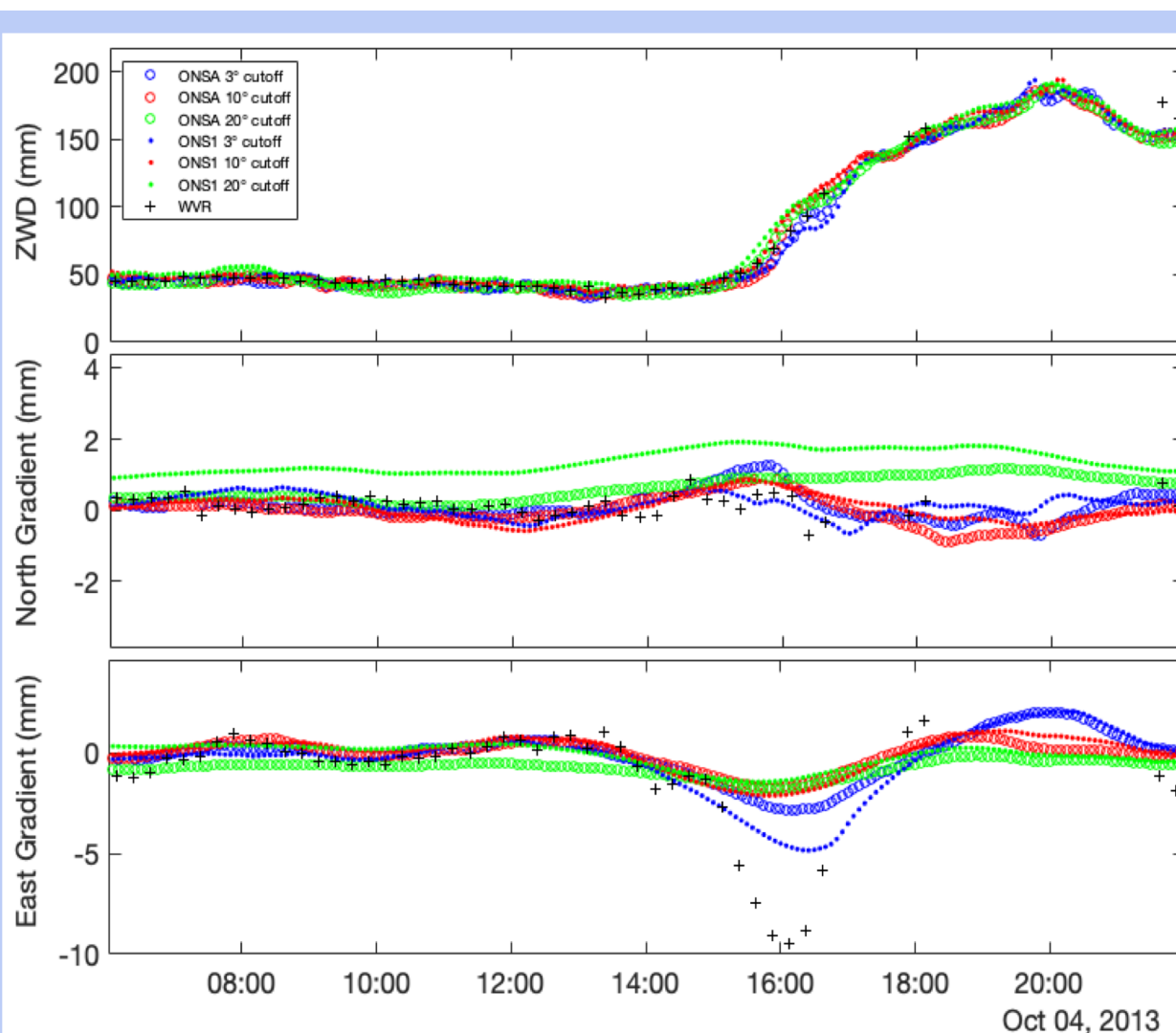


Fig. 7. A very distinct warm front passed the site on the 4th of October, 2013. A change in the ZWD from 50 mm to 200 mm in just 4 h is rather unusual, and in fact the west gradient of 10 mm observed by the WVR is one of the largest during the four year period. Comparing the different GPS solutions it is a bit surprising that the east gradients for ONSA and ONS1 differ significantly between the 3° cutoff angle solutions, although they agree better with the WVR gradients compared to the gradients from the solutions using the other cutoff angles. The difference between ONSA and ONS1 may call for additional studies. We note that the north gradients estimated using the 20° cutoff angle seem inaccurate.

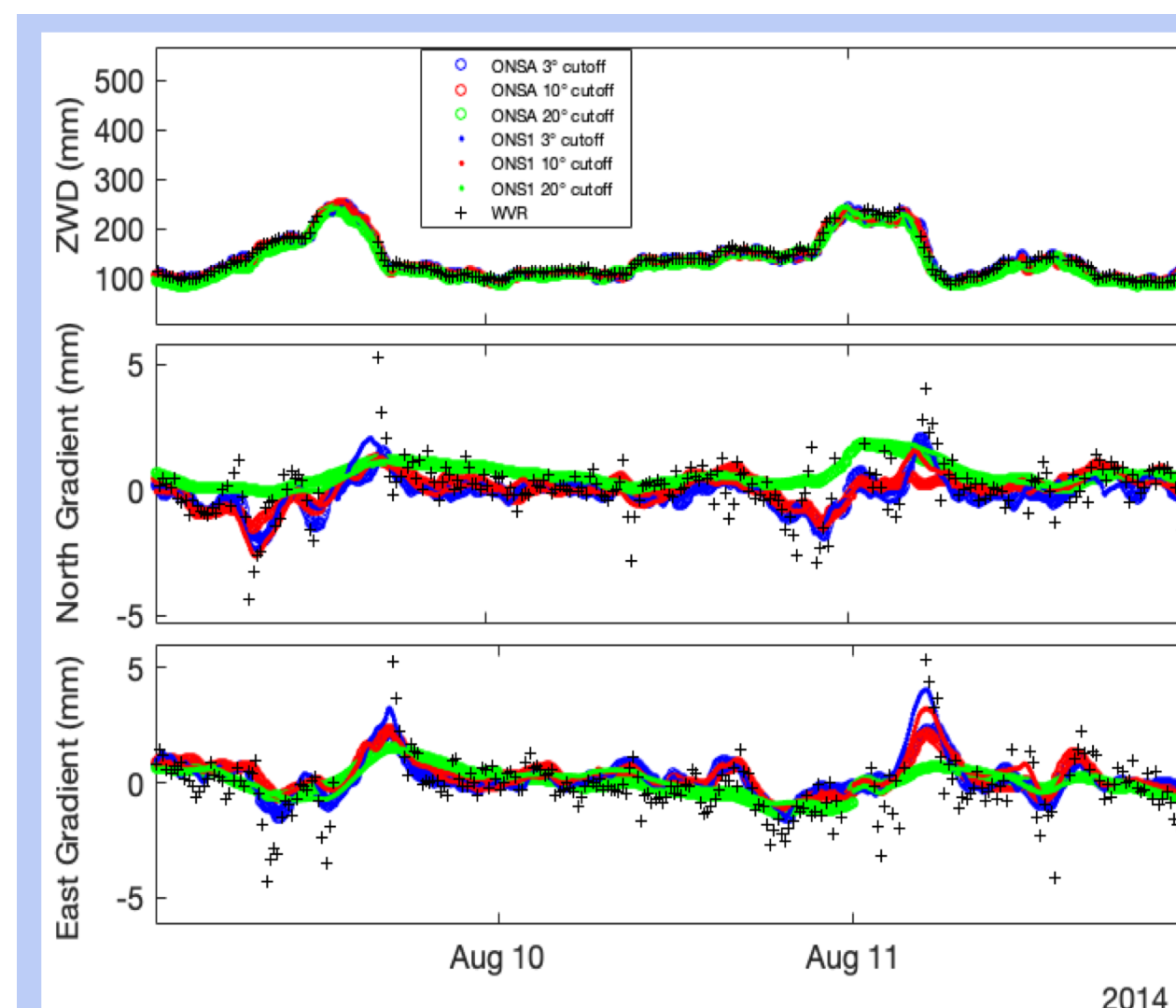


Fig. 8. Two cold front passages are shown in this example: in the afternoon of 9th of August and in the morning of 11th of August. There are also significant gradients detected in the GPS solutions, south gradients before the cold front arrives on the 9th of August, using the 3° and 10° cutoff angles, which are supported by the WVR data. Also in this example the gradients estimated by the 20° cutoff angle solution show significant differences compared to the other time series. The figure also depicts that the east gradients from ONS1 are larger than those from ONSA at the front passage around 5 UT of the 11th of August.

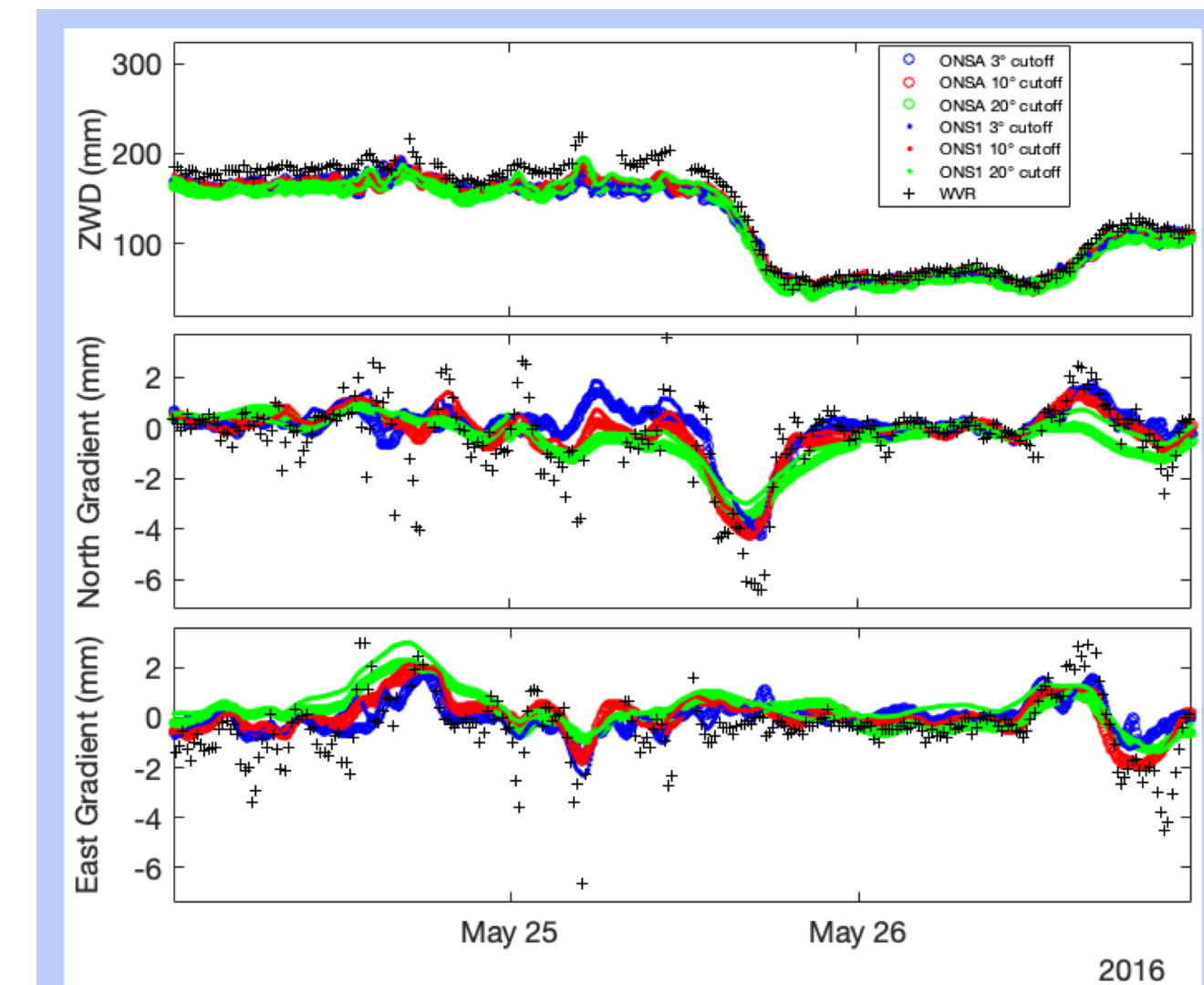


Fig. 9. In this example the estimated gradients from all GPS solutions and the WVR all have large values in the south direction around 17 UT on 25th of May 2016. Before the cold front arrives at the station we also see variability in the estimated gradients, and especially in the WVR time series. Although the WVR gradients correlate with the GPS gradients we cannot rule out that rain or large liquid drops have had a negative impact on the accuracy of the WVR gradients. This may be in combination with small scale structures in the atmosphere implying that the GPS and WVR observations sample different atmospheric paths that are not well described by the linear model.

## Conclusions (continued)

Related to these observations we conclude that for the weather conditions at this site the passage of frontal systems is the cause for the largest gradients in the atmosphere. A consequence is that they are not long lived, typically just a few hours or less.

The elevation cutoff angle has a significant impact on the estimated gradients. We interpret that this is a combined effect of a weaker geometry for higher cutoff angles and systematic effects in the electromagnetic environment of the antenna. We do not recommend elevation cutoff angles as high as 20° when there is a goal to estimate accurate horizontal gradients. This conclusion may change if multi GNSS is used, providing more satellites meaning more observations and a better geometry. We recommend further studies related to these issues.

## References

- Bar-Sever, Y.-E., Kroger, P. M., and Börjesson, J. A. (1998). Estimating horizontal gradients of tropospheric path delay with a single GPS receiver, *J. Geophys. Res.*, 103, pp. 5019–5035, <https://doi.org/10.1029/97jb03534>.
- Boehm, J. and Schuh, H. (2007) Troposphere gradients from the ECMWF in VLBI analysis, *J. Geod.*, 81, pp. 403–408, <https://doi.org/10.1007/s00190-007-0144-2>.
- Elgered, G., Ning, T., Forkman, P., and Haas R. (2019). On the information content in linear horizontal delay gradients estimated from space geodesy observations, *Atmos. Meas. Tech.*, 12, pp. 3805–3823, <https://doi.org/10.5194/amt-12-3805-2019>.
- Graffigna, V., Hernández-Pajares, M., Gende, M. A., Azpilicueta, F. J., and Antico, P. L. (2019). Interpretation of the tropospheric gradients estimated with GPS during Hurricane Harvey, *Earth and Space Science*, 6, <https://doi.org/10.1029/2018EA000527>.
- Morel, L., Pottiaux, E., Durand, F., Fund, F., Boniface, K., de Oliveira, P. S., and Van Baelen, J. (2015). Validity and behaviour of tropospheric gradients estimated by GPS in Corsica, *Adv. Space Res.*, 55, pp. 135–149, <https://doi.org/10.1016/j.asr.2014.10.004>.